



Synthesis and Characterization of Lanthanum Oxide and Lanthanum Oxide Carbonate Nanoparticles from Thermalizes of [La(acacen)(NO₃)(H₂O)] Complex

HAMIDEH SARAVANI* and MALIHEKHA JEHALI

Department of Chemistry, University of Sistan and Baluchestan, P.O. Box 98135-674, Zahedan, Iran.

*Corresponding author E-mail: saravani@chem.usb.ac.ir

<http://dx.doi.org/10.13005/ojc/320156>

(Received: October 07, 2015; Accepted: February 25, 2016)

ABSTRACT

In this investigation, we report facile synthesis of transition metal oxides (La₂C₂O₅ and La₂O₃) as nanoparticles. The process contained two steps: first preparation of complex [La(acacen)(NO₃)(H₂O)](1) where acacen= acetylacetonatoethylenediamine. Then the precursors were calcination. In first step, complex (1) synthesized using a methanolic solution of La (NO₃)₃ and acetylacetonatoethylenediamine. Then desired product was collected by suction filtration and characterized using Fourier transform infrared (FT-IR), Ultra Violet-Visible (UV-vis) spectroscopy and cyclic voltammetry (CV) method for electrochemical studies. The next step to prepare nanoparticles, amount of compound (1) put in silica gel and oleic acid solution for 4-hours. Then compound (1) was placed in a furnace with a temperature of 600, 700, 800 and 900°C. After calcination of title compound, this sample studied using XRD (X-ray Diffraction) and SEM (Scanning Electron Microscopy) techniques. Particle size for several diffraction and average crystallite size were measured from the XRD data based on Debye- Scherrer equation. The X-ray diffraction patterns at room temperature revealed that, highly pure and crystallized Lanthanum oxide nanoparticles as La₂C₂O₅ and La₂O₃ formula with orthorhombic phases in 600°C and 900°C respectively, with an average particle size of about less than 100nm for both nano-oxide. SEM figure show that the particles have same morphology with a uniform porous surface.

Key words: Nanoparticle, X-ray Diffraction, Morphology, Orthorhombic. (Footnotes).

INTRODUCTION

In recent years, the synthesis of inorganic materials with specific size and morphology has attracted considerable attention. Their excellent

physical and chemical properties in various fields, such as solar cells, catalysis, photo detectors, sensors, light emitting diodes and laser communication, have made them attractive¹⁻⁴ and promising materials. It is well documented that materials with nano-scale grain

size show different properties relative to the same material in bulk form⁵⁻⁷. Preparation of various nano-materials have many different synthetic approaches such as chemical vapor deposition (CVD), thermal evaporation, chemical bath deposition, laser ablation, hydrothermal, homogeneous precipitation in an organic matrix, sonochemical and sol-gel method⁸⁻¹⁵. The synthesis, production and manipulation of materials on the Nano scale is one of the favorite areas of research which also attracts the industrialists for designing and fabricating new functional materials with novel special properties^{1,2}. Among the lanthanides, lanthanum has been

extensively examined for its unique properties⁷⁻¹² and lanthanum has been synthesized in various compositions such as $\text{La}(\text{OH})_3$ ¹³, LaF_3 ⁵, $\text{La}_2(\text{CO}_3)_3$ ¹⁴, LaPO_4 ¹⁵⁻¹⁷, LaBO_3 ¹⁸, LaOF ¹⁹, $\text{La}_2\text{Sn}_2\text{O}_7$ ²⁰, La_2O_3 ²¹ nanoparticles.

Lanthanum oxide (La_2O_3) powders have a lot of attractive properties for industrial and technological applications such as: 1- Nanometer lanthanum oxide can be used in piezoelectric materials to increase product piezoelectric coefficients and improve product energy conversion efficiency; 2- Nano-lanthanum oxide can be used for the manufacture of precision optical glass, high-refraction optical fiber, all kinds of alloy materials; 3- Nano-lanthanum oxide can be used for the preparation of organic chemical products catalysts, and in automobile exhaust catalyst; Nanometer Lanthanum oxide can improve the burning rate of propellant, is a promising catalyst; 4- As regards the photoelectric conversion efficiency of nano-lanthanum oxide is high, it can be used in light-converting agricultural film; 5- Also, nano-lanthanum oxide can be used in electrode materials and in light-emitting material (blue powder), hydrogen storage materials, laser materials etc.

In the present work, we report the synthesis of $[\text{La}(\text{acacn})(\text{NO}_3)(\text{H}_2\text{O})](1)$, then this compound has been converted to Lanthanum oxides nanoparticle as La_2CO_5 at 600°C and La_2O_3 at 900°C .

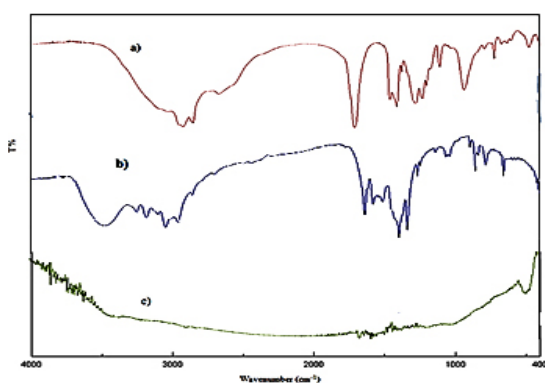


Fig. 1: FT-IR spectra of a) oleic acid b) $[\text{La}(\text{acacn})(\text{H}_2\text{O})(\text{NO}_3)]$ (1) c) La_2O_3 (3) in KBr pellets

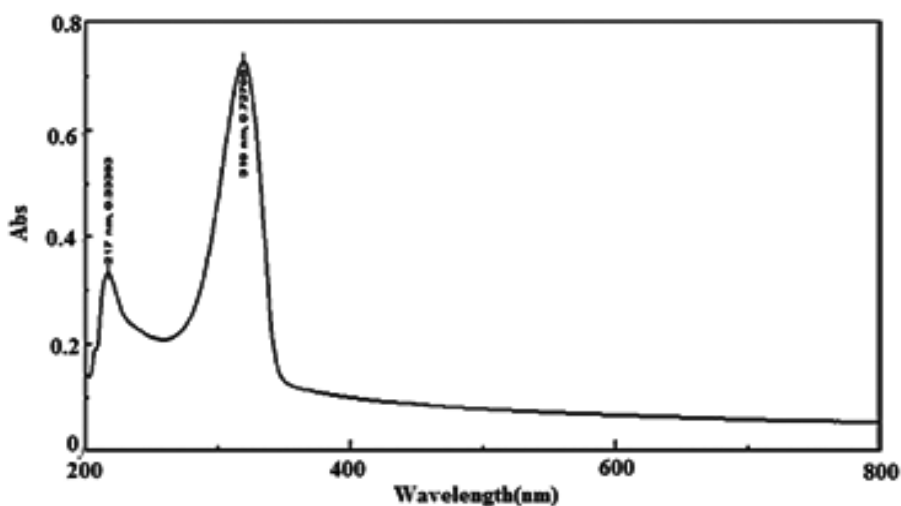


Fig. 2: UV-vis absorption spectra of $[\text{La}(\text{acacn})(\text{H}_2\text{O})(\text{NO}_3)](5 \times 10^{-5}\text{M})$ in DMF(1)

EXPERIMENTAL

Material and Characterization

All chemicals and solvents were reagent grade or better, obtained from Merck, and used without further purification.

Infrared spectra ($4000\text{--}250\text{ cm}^{-1}$) of solid samples were taken as 1% dispersion in KBr pellets using a JASCO FT-IR 460 PLUS. Electronic absorption spectra in DMF solution were taken at room temperature on a JASCO 7850 spectrometer. Cyclic voltammograms were recorded using a SAMA500. Three electrodes were utilized in this system: a glassy carbon working electrode, a

platinum wire auxiliary electrode and an Ag wire reference electrode. The glassy carbon working electrode was manually cleaned with 1- μm diamond polish prior to each scan. The supporting electrolyte, 0.1 M tetrabutylammoniumhexafluorophosphate (TBAH), was recrystallized twice from ethanol-water (1/1) and vacuum-dried at 110°C overnight. A sweep rate of $100\text{--}500\text{ mVs}^{-1}$ was used for all the scans. Ferrocene was used as an internal standard to compensate for the junction potential variability among experiments.

The thermal behavior was measured with a PL-STA 1500 apparatus. XRD analysis was conducted on a Philips diffractometer of X'pert

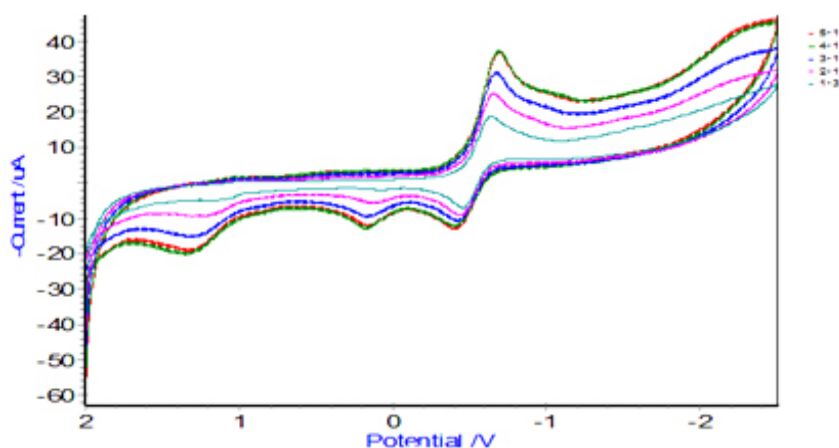


Fig. 3: Cyclic voltammogram of $[\text{La}(\text{acacen})(\text{H}_2\text{O})(\text{NO}_3)](1)$ in DMF, 0.1 M TBAH as a supporting electrolyte

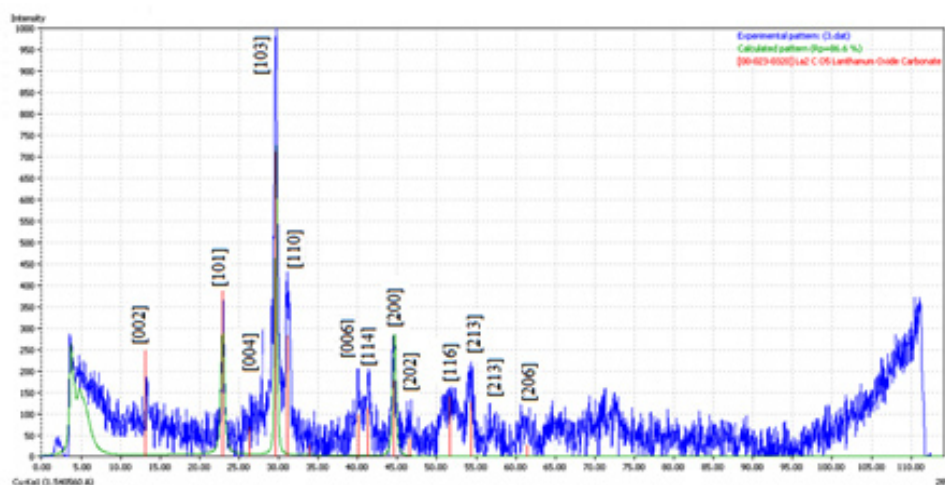


Fig. 4: XRD pattern of La_2CO_5 at 600°C , compared with standard sample

final products were collected and washed with distilled water and absolute ethanol several times, dried in air and kept for further characterization.

RESULTS AND DISCUSSION

FT-IR spectroscopy

The broadbands at 2600-3000 cm^{-1} and 1712 cm^{-1} assigned to stretching vibration of O-H and C=O groups in oleic acid respectively (Fig 1a). As it can be observed in Fig.1 all the bands of the oleic acid and [La (acacen) (H₂O) (NO₃)](1) were disappeared when the product was calcinated in 900 °C (Fig1c) and only broad band was appeared that attributed to lanthanum oxide (Fig1c). The strong band at 500 cm^{-1} is assigned to the $\nu(\text{La-O})$, indicating formation of La₂O₃(3).

Strong bands at 1585, 1505 and 1625 cm^{-1} , related to the stretching vibrations of C = C, C = N, C = O can be shared on acacen ligand. And stretching frequency observed in the 1374 cm^{-1} attributed to NO₃ group²². Weak absorptions in the region 3158 and 3226 cm^{-1} assigned to N-H vibration of the acacen ligand^{22,23}.

FT-IR spectra of oleic acid showed in the Fig1b. The broadband observed at 2925-2000 cm^{-1} , attributed to overlap of stretching vibration frequency

Table 1: Particle and average crystallite size of La₂CO₅ in absence of oleic acid at 600°C

2 θ	B	Size (nm)	Average size (nm)
3.71	0.006	23.1	25.02
22.92	0.009	17.32	
29.67	0.005	34.65	

Table 2: Particle and average crystallite size of La₂CO₅ in presence of oleic acid at 600°C

2 θ	B	Size (nm)	Average size (nm)
3.77	0.007	19.8	15.58
22.95	0.013	11.55	
29.90	0.010	15.4	

of the acidic OH screw with CH bands. The bonds observed at 3006 cm^{-1} , 1711 cm^{-1} , 1378 cm^{-1} and 1465 cm^{-1} assign to CH, C=O, CH₂ and CH₃ groups, respectively.

Electronic Excitation Study

The electronic spectrum of the [La (acacen) (H₂O) (NO₃)] (1) showed in Fig2. Absorption bands in 217 and 319 nm can be assigned to the intraligand $\pi \rightarrow \pi$ transition of the aromatic ring and $\pi \rightarrow \pi$ transition of the acacen and nitrate ligands, respectively. There was any transition in visible region due to Lanthanum (III) has d⁰ electron configurations.

Electrochemical Studies

Cyclic voltammetry was performed in an DMF solution of [La(acacen)(H₂O)(NO₃)](1) with 0.1M TBAH as a supporting electrolyte at scan rate 100-500 mV s^{-1} (Fig. 3). In this voltammogram, two quasi-reversible reduction couples at -0.458 and -0.690 V are assigned to the reduction of acacen ligand, by analogy to other acacen complexes²⁴. In comparison with free acacen, the reduction couples shift to more positive potentials due to the coordination of acacen ligand to the La(III) center.

X-ray diffraction

Fig 4 and 5 show the representative XRD pattern of La₂CO₅ in the absence and presence of oleic acid at 600°C respectively. It is obvious that all the diffraction peaks can be indexed to orthorhombic phase La₂CO₅ (LCS D Card Number 4242). Compared with the standard diffraction pattern. Maximum diffraction observed at $2\theta = 29.67^\circ$ and (103) as miller indices, Fig 4. In addition, the distance between crystalline planes is $d = 3\text{\AA}$ ²⁵. Also the intense and sharp diffraction peaks with any signals of impurities were attributed to high purity of the product. As can be seen in Fig 5. maximum

Table 3: Particle and average crystallite size of La₂O₃ at 900°C

2 θ	B	Size (nm)	Average size (nm)
15.94	0.015	86.62	56.43
28.68	0.019	36.47	
39.80	0.006	46.2	

diffraction is in $2\theta=29.90^\circ$ with (103) as miller indices and $d=3.1 \text{ \AA}$, with addition of oleic acid.

Also particle size for several diffraction and average crystallite size that were measured from the XRD data based on Debye- Scherrer equation for La_2CO_3 in absence and presence of oleic acid

at 600°C show in Table 1 and 2 respectively. As can be seen in Table 1, the compound has nano-sized in the range of nanoparticles (below 100 nm)²⁵.

$[\text{La}(\text{acacen})(\text{H}_2\text{O})(\text{NO}_3)]$ calcinated to La_2O_3 in a furnace at 900°C . Fig 6. Show XRD pattern of La_2O_3 at 900°C . Nano lanthanum oxide

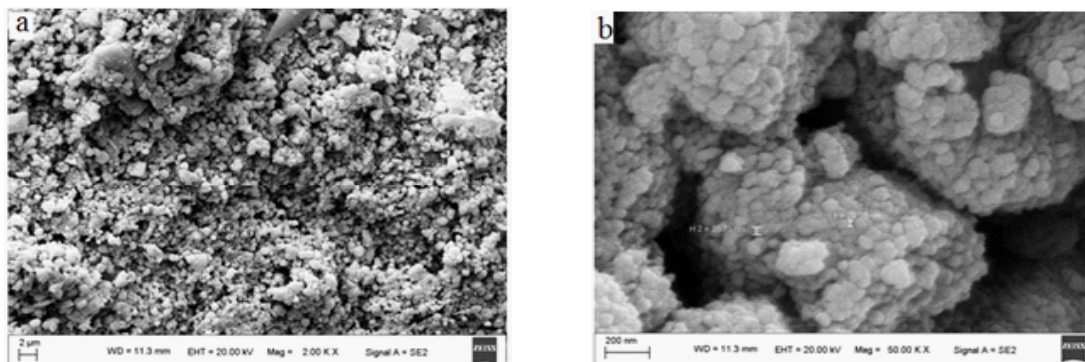


Fig. 7: SEM images of La_2CO_5 at 600°C

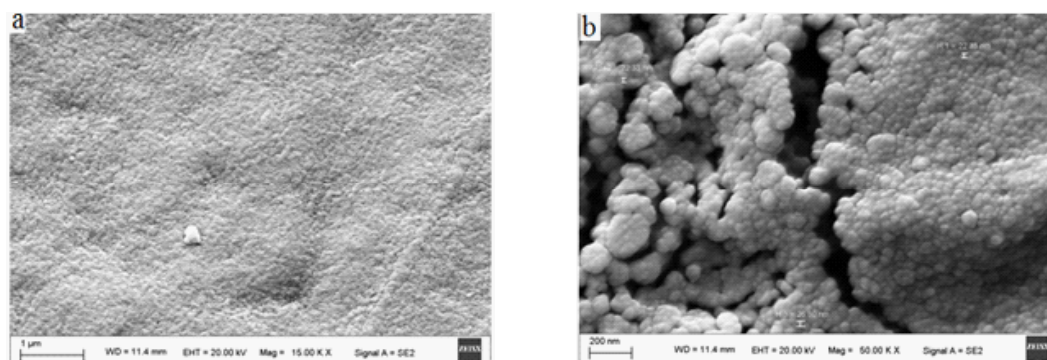


Fig. 8: SEM images of La_2CO_5 in presence of oleic acid at 600°C

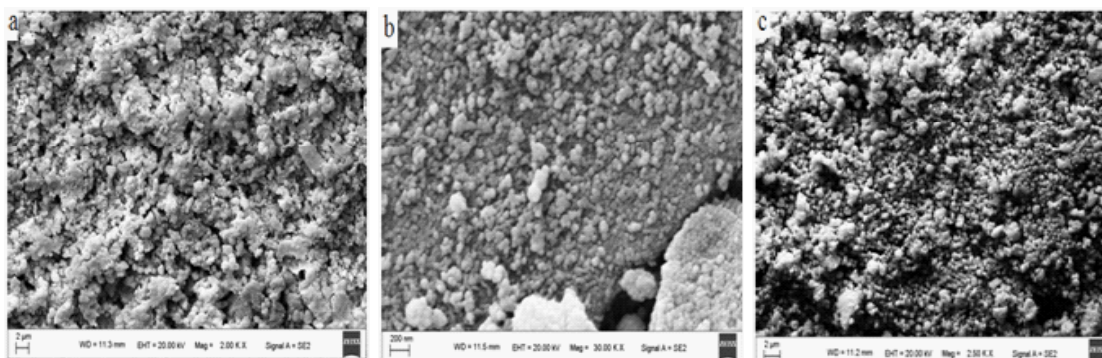


Fig. 9: SEM images La_2O_3 at a= 700 , b= 800 , c= 900°C

has orthorhombic system with diffraction maximum intensity at $2\theta = 39.80^\circ$ and Miller indices (1 1 1) with distance between the plates $d = 2.98 \text{ \AA}$ (Table 3).

Surface morphology

The morphology of the La_2CO_5 nanoparticles was characterized using scanning electron microscope (SEM) at 600°C . Fig. 7 and 8 show the SEM images of La_2CO_5 in absence and presence of oleic acid respectively. As can be seen the images are clear examples and nano-carbonate oxide relatively spherical, porous and beneath the high porosity for use as a catalyst for much is suitable. So that the particle size is found 29.0-35.73 nm and 22.33-26.89 nm respectively that in order to the effect of surfactants on the image more uniform and stronger link between particle surface area that can provide a better view.

La_2O_3 have spherical shape with porous surface and particle size 24.56- 13.40 nm. Fig 9.

CONCLUSION

Metals, rare earths, has a strong tendency to combine with non-metallic elements such as oxygen, nitrogen, carbon and hydrogen, and various factors such as geometry and central atom, the structural features of the ligand molecules, with a solvent can play key roles in the formation of structures them.

The nano-sized particles have different properties than the bulk material can

be explained by the fact that the smaller the particle size, the number of atoms will be higher. As a result, the surface energy of atoms within a material volume with a different energy and this will cause different properties. The unique properties of nanometer particles, not only because of their high level, but also for other reasons such as changes in the crystal lattice, the link between nuclear energy and so is relevant. It should be noted that the production of nano-materials and the geometric arrangement of atoms is consistent with the changes in particle size, particle size reduction increases the effect of the level. Increased surface to volume ratio of nanoparticles causes the atoms in the surface atoms than the particle size, the particles have physical properties. This feature greatly increases the reactivity of nanoparticles.

In summary, we prepared Lanthanum oxide nanoparticles in the presence and absence of Oleic acid as a surfactant. The size of these nanoparticles was measured using XRD and SEM. The images of nano-lanthanum oxide at elevated temperatures ($600, 700, 800$ and 900°C) observed that in all the images of the particles are almost spherical, with uniform and porous morphology and particle size are almost identical.

ACKNOWLEDGMENTS

The authors are grateful to the University of Sistan and Baluchistan University for partial financial support.

REFERENCES

- Singh, V.P.; Singh, R.S.; Thompson, G.W.; Jayaraman, V.; Sanagapalli, S.; Rangari, V.K. *Sol. Energy Mater. Sol. Cells* **2004**, *81*, 293-303
- Shahverdizadeh, G.H.; Morsali, A. *J. Inorg. Organomet. Polym.* **2011**, *21*, 694-699
- Payehghadr, M.; Safarifard, V.; Ramazani, M.; Morsali, A. *J. Inorg. Organomet. Polym.* **2012**, *22*, 543-548.
- Hashemi, L.; Hosseini, M.; Amani, V.; Morsali, A. *J. Inorg. Organomet. Polym.* **2013**, *23*, 519-524.
- Marban, G.; Lopez, A.; Lopez, I.; Valdes-Solis, T. *Appl. Catal. B Env.* **2010**, *99*, 257
- Valdes-Solis, T.; Marban, G.; Fuertes, A.B. *Catal. Today* **2006**, *116*, 354-360.
- Jones, S.D.; Neal, L.M.; Everett, M.L.; Hoflund, G.B.; Weaver, E.H.H. *Appl. Sur. Sci.* **2010**, *256*, 7345-7353.
- Wu, Y.; Yang, P. *Chem. Mater.* **2000**, *12*, 605-607.
- Iijima, S. *Nature* **1991**, *354*, 56-58.
- Morales, A.M.; Lieber, C.M. *Science*. **1998**, *279*, 208-211.
- Suciu, C.; Gagea, L.; Hoffmann, A. C.; Mocean, M. *Chem. Eng. Sci.* **2006**, *61*, 7831-

- 7835.
12. Salavati-Niasari, M.; Hosseinzadeh, G.; Davar, F. *J. Alloys Compd.* **2011**, *509*, 134-140.
 13. Ranjbar, M.; Çelik, Ö.; Mahmoudi Najafi, Sheshmani, S.H., Akbari Mobarakeh, N. *J. Inorg. Organomet. Polym.* **2012**, *22*, 837-844
 14. Ranjbar, M.; Malakooti, E.; Sheshmani, S. *J. Chem.* **2013**, Vol. 2013, Article ID 560983, 6 pages doi: 10.1155/2013/560983
 15. Khorasani-Motlagh, M.; Noroozifar, M.; Ahanin-Jan, A. *J. Iran. Chem. Soc.* **2012**, *9*, 833-839.
 16. Averbuch-Pouchatand M. T.; Durif, A. World Scientific Publishing Co. Pte.Ltd., Singapore City, **1996**.
 17. Hammas, I.; Horchani-Naifer K.; Ferid, M. *Journal of Rare Earths*, **2010**, *28*, 3, 321-328.
 18. Meiser, F.; Cortez, C.; Caruso, F. *Angewandte Chemie*, **2004**, *43*, 44, 5954-5957.
 19. Onoda, H.; Nariai, H.; Moriwaki, A.; Maki, H.; Mo-tooka, I. *J. Mat. Chem*, **2002**, *12*, .6, 1754-1760 .
 20. Onoda, H.; Funamoto, T. *Adv. Mat. Phy. and Chem*, **2012**, *2*, .1, 50-54.
 21. Rajesh, K.; Shajesh, P.; Seidei, O.; Mukundan, P.; Warriar, K. G. K. *Adv. Fun. Mat*, **2007**, *17*, .10, 1682-1690
 22. Onoda, H.; Taniguchi, K.; Tanaka, I., *Micro and Meso. Mat.*, **2008**, *109*, .1-3, 193-198.
 23. Alkadasi, N. A. N.; *Orient. J. Chem.*, **2014**, *30*(3), 1179-1182.
 24. Onoda, H.; Matsui, H.; Tanaka, I. *Mat. Sci. Eng. B*, **2007**, *141*, No. 1-2, 28-33.
 25. Parimalagandhi, K.; Vairam, S.; *Orient. J. Chem.*, **2014**, *30*(4), 1957-1963.